

# Search for Exoplanets with a Possible Surface Water Ocean <sup>†</sup>

Roland Novak <sup>1,\*</sup>, Balazs Bradak <sup>1</sup>, Jozsef Kovacs <sup>2</sup> and Christopher Gomez <sup>1,3</sup><sup>1</sup> Faculty of Oceanology, Kobe University, 5-1-1 Fukaeminami-machi, Higashinada-ku, Kobe 658-0022, Japan<sup>2</sup> Independent Researcher<sup>3</sup> Faculty of Geography, Universitas Gadjah Mada, Yogyakarta, Indonesia

\* Correspondence: rolandnovak95@gmail.com

<sup>†</sup> Presented at the 2nd Electronic Conference on Universe, 16 February–2 March 2023; Available online: <https://ecu2023.sciforum.net/>.

**Abstract:** In this work, we examined characteristics of the currently confirmed exoplanet population in order to characterize some of the crucial parameters for ocean formation. Two correlation heatmaps were created, one for the exoplanets in general, and one for exoplanets that can be found in the habitable zone by the calculations. Based on these, we found possible associations between planetary radius/mass, stellar metallicity, and multiple characteristics. We also proposed plans for further studies of possible proxies for exoplanetary ocean exploration.

**Keywords:** exoplanets; planetology; oceanology; exoplanet habitability

## 1. Introduction

Surface habitability on exoplanets is a major question in extrasolar research. Oceans in general, and the interaction between landmasses and water were crucial driving forces during the biological evolution on Earth. As analogs to early Earth, “water worlds” outside our Solar System may also harbor life, which conjectures turned into the main triggers of the intensive search for exoplanets. In the last decades, multiple devices were used to search for exoplanets around stars ([1–3]), and this gathered information can be found in various databases, e.g., NASA’s Exoplanet Archive [4].

Before the recent successful exploration of the first exoplanets with high water content around Kepler-138 [5], multiple hypostases, with diverse focuses and approaches, were created on how to search for ocean planets [6], from the early conditions of star systems [7], through the diversity of ocean-planets around M-type dwarfs [8], to the planet surface-sea interaction and ocean dynamics on these planets [9]. Along with the theories, an index was created to describe the similarity of exoplanets compared to Earth [10]. This index is an alternative to the habitable zone parameters, which defines the domains around stars, where liquid water is possible to exist on the surface [11].

Our study aims to summarize and examine the currently available exoplanetary data and show trends and connections in planetary characteristics as potential proxies of the surface ocean in the exoplanetary environment. It may help to reveal potential factors in ocean forming and help to reveal candidate star systems for future surveys.

## 2. Data and Methods

The research was executed in the following steps:

Step 1. To examine all the available exoplanets, NASA’s Exoplanet Archive was accessed [4]. The database consists of 5187 confirmed exoplanets, some of them in the same star system. During the first approach, unfiltered data was used. Secondly, the database was filtered to the planets, which are in the habitable zone (see below).

Step 2. Calculation of the habitable zone (HZ) [12]:

**Citation:** Novak, R.; Bradak, B.; Kovacs, J.; Gomez, C. Search for Exoplanets with a Possible Surface Water Ocean. *2023*, *3*, x.

<https://doi.org/10.3390/xxxxx>

Published: 15 February 2023



**Copyright:** © 2023 by the authors. Submitted for possible open access publication under the terms and conditions of the Creative Commons Attribution (CC BY) license (<https://creativecommons.org/licenses/by/4.0/>).

$$d = \left( \frac{L/L_{\odot}}{S_{eff}} \right)^{0.5} AU \tag{1}$$

where  $S_{eff}$  is the calculated insolation flux, reaching the planet’s upper atmosphere and  $L/L_{\odot}$  is the star’s luminosity compared to the Sun’s.  $S_{eff}$  can be calculated for different planet conditions, but generally, it is advised to calculate for the recent Venus and early Mars states, which are the most optimistic approaches considering habitability ([13,14]). This equation was originally used for F, G, K, and M-type stars ( $2600\text{ K} \leq T_{eff} \leq 7200\text{ K}$ ), but in this paper, the habitable zone limits of all stellar types were calculated by this formula. This showed the zones which are perhaps optimal to allow the appearance of liquid water. Further studies will require a different approach for the few upper main-sequence stars and other stellar objects.

Step 3. Searching for trends in the unfiltered and filtered data: to assess the connection between the parameters, the Pearson correlation coefficient ( $r$ ) of the planetary and stellar characteristics was calculated. The correlation matrices and heatmaps were created in a Python environment.

Step 4. The review of the connection between planetary characteristics to assess their influence on the possibility of a liquid water ocean on an exoplanet’s surface.

### 3. Results and Discussion

#### 3.1. Heatmap Analysis of Various Parameters

The heatmap analysis of the unfiltered data (Figure 1a) can be summarized as the following. Non-negligible (inverse) correlations can be found between the planetary radius and the planetary mass ( $r = 0.32$ ), planetary radius and stellar mass ( $r = 0.29$ ), planetary radius and the number of planets in the system ( $r = -0.24$ ), and planetary radius and orbital eccentricity ( $r = 0.42$ ). The first correlation arises because more massive planets tend to be larger in radii, and the second correlation is likely the byproduct of the transit observational method since planets with larger radii are easier to find around more luminous stars than fainter ones. The last two (anti)correlations are also present with a stronger anticorrelation in the case of habitable zone planets (Figure 1b), so it might be a general trend in star systems, not necessarily connected to the occurrence of oceans/habitability zones, but we will mention them in the next subsections.

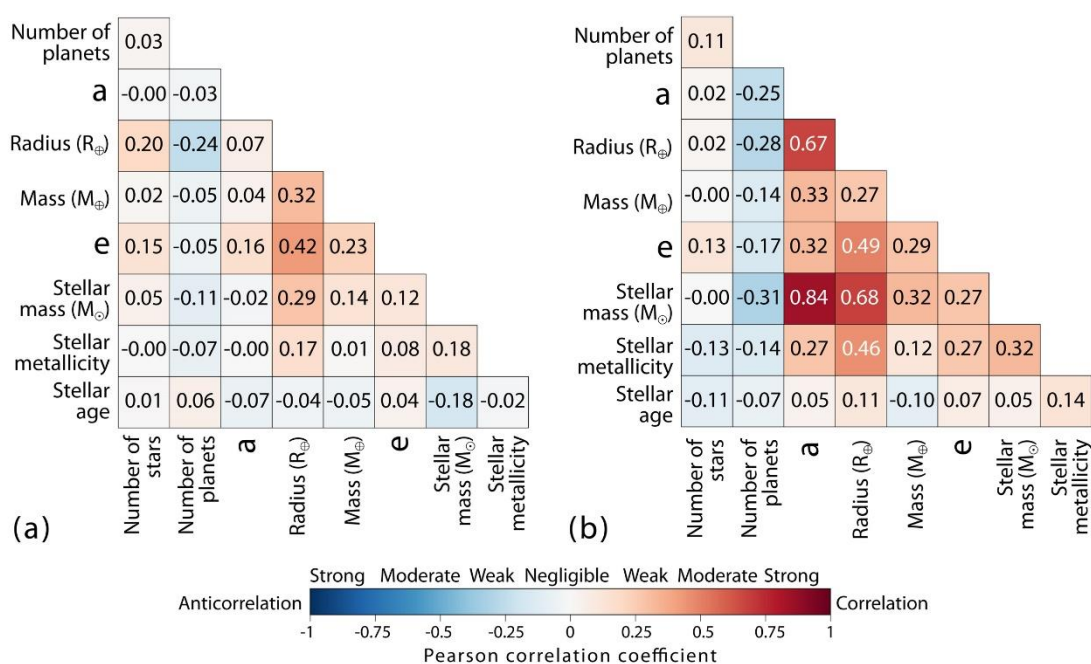


**Figure 1.** The correlation heatmap of possible ocean-forming factors, with all the confirmed exoplanets (5186) (a); and the correlation heatmap of the possible ocean-forming factors, with all the exoplanets, which can be found in the habitable zone by the calculation (230). (b) Abbreviations on the axes:  $a$ —semi-major axis (AU);  $e$ —orbital eccentricity.

The analysis of the filtered database (contains only the planets which can be found in the habitable zone) indicated the following (Figure 1b). Multiple non-negligible correlations and anticorrelations can be found, mainly along the same parameters as before, just with stronger correlation or inverse correlation. The main correlations can be found between the planet radius-semi major axis ( $r = 0.67$ ), planetary mass-semi major axis ( $r = 0.33$ ), orbital eccentricity-semi major axis ( $r = 0.32$ ), stellar mass-semi major axis ( $r = 0.84$ ), orbital eccentricity-planetary radius ( $r = 0.49$ ), stellar mass-planetary radius ( $r = 0.68$ ), stellar metallicity-planetary radius ( $r = 0.46$ ) and the main anticorrelations were between stellar mass-number of planets in the system ( $r = -0.31$ ), and planetary radius-number of planets in the system ( $r = -0.28$ ). The connection between the planetary characteristics (planetary radius, planetary mass) and the semi-major axis ( $r = 0.67$  and  $r = 0.33$ ) in the habitable zone is quite peculiar since it is not similar to the Solar System.

### 3.2. Evaluation of the Connection between Various Parameters

The heatmap analysis showed that certain parameters statistically relate to a bigger number of other parameters. Hypothetically, it may indicate their significance e.g., in the formation of surface oceans. Such parameters are introduced below.

#### 3.2.1. The Planetary Radius

On the heatmaps, the most apparent feature is the connection between the planetary radius and various other parameters, such as stellar mass, semi-major axis, orbital eccentricity, stellar metallicity, and the number of planets in the system (Figure 1a,b).

Radii (and masses) of celestial bodies separate them along distinct physical characteristics. Bigger planetary bodies may host liquid water oceans if other habitability conditions are given, and the planetary radius is generally a good first approach to determining an exoplanet's main type, the more that it is possible to measure it with the transit search method.

There is a moderate correlation ( $r = 0.67$ ) between the planetary radius and planetary semi-major axis in the habitable zones (Figure 1b), but this correlation is almost zero ( $r = 0.07$ ) in the case of unfiltered data (Figure 1a). The latter low correlation can be explained by the high variety of stellar systems and planetary formations in the exoplanet population: multiple hot Jupiters with small semi-major axis and high radius/mass (e.g., KELT-9b) [15], and terrestrial planets with relatively higher semi-major axis and low mass (Kepler-37b) are known. For planets in the habitable zone, the existing correlation is not consistent with the Solar System's habitable zone. In any case, our current understanding of planetary formation (planetesimals with greater semi-major axes can acquire more material because they are further and further away from the ice-line of the star [16]) generally tends to support this correlation. Perhaps star systems, with less massive planets in the inner HZ and more massive planets in the outer HZ are more common. This would be helpful since a bigger planet can withhold a significantly denser atmosphere (hence a larger radius too), which can act as a countermeasure against the lower insolation and can help to preserve a liquid water ocean.

The case of the correlation between the planetary radius and orbital eccentricity ( $r = 0.49$ ) is examined in the next subsection, from the viewpoint of mass. The stronger correlation with the radius is mayhaps present due to the presence of gas planets in the HZ, with a heated and inflated atmosphere around M stars.

The moderate correlation ( $r = 0.46$ ) between stellar metallicity and planetary radius follows the expectations. Stars with various metallicities (the abundance of elements heavier than hydrogen and helium) are categorized into Population I, II, and III, which shows

their metal abundances decreasing, and their age increasing with higher population numbers. Metallicity is thought to be an important parameter: since the uppermost layers of stars mix rarely with deeper layers, the observed metallicity gives away a hint about the primordial environment of the star system [17]. During planet formation, in older star systems with lower metallicities, it is much harder for a protoplanet to accumulate enough material to reach the sufficient mass for a Jupiter-like gas giant or even the mass of a super-Earth ([18,19]). Earlier studies also showed that there is a correlation between higher stellar metallicities and planet appearance frequency [20], but in our case, no significant correlation was found.

The strongest anticorrelation (still only a weak association) can be found between the planetary radius and the number of planets in the system ( $r = -0.28$ ; and  $r = -0.24$ , at the unfiltered data). From the database, some systems with the most confirmed exoplanets were examined to test this particular correlation: these are in order Kepler-90 (8 planets), TRAPPIST-1 (7), HD 10180 (6), and HD 219134 (6). Of these 27 planets, most of them (19) are Earth- or Neptune-sized planets (in the case of TRAPPIST-1, all of them), with just a small number of Jupiter-sized planets. Since exoplanets with larger radii are easier to find, this anticorrelation is surprising. Whether this anticorrelation is due to orbital, formation, or observational bias effects, is yet to be answered.

Lastly, it is highly likely that the correlation between the stellar mass and planetary radius (0.68) is the byproduct of the transit detection method [21], since around more luminous stars, it is easier to detect planets with larger radii because a transit of a small planet causes only a minor fluctuation in its star brightness.

### 3.2.2. Semi-major Axis

There is a weak association ( $r = 0.33$ ) between the planetary mass and planetary semi-major axis in the habitable zones (Figure 1b), but no association was recognized using the unfiltered data (see above; Figure 1a).

Many extrasolar planets with relatively short orbital periods (20 days or less) and small semi-major axis, tend to have low eccentricities [22], and a weak correlation ( $r = 0.32$  in the case of planets in the HZ, Figure 1b) in the database also assures this. This is because of their proximity to their parent star, which causes tidal circularization on large time-scales ([23,24]). Even though these lower eccentricities would be ideal to avoid the in-out movement from the habitable zone, the habitability of these planets is strongly questioned. The negative effect of the tidal locking scenario (which occurs in these closely packed systems [25]) would be immense temperature differences between the day and the night sides, which can cause the hypothetical ocean to boil on one side, and completely freeze on the other. The long-time stability of the atmospheres is also endangered in these cases ([26,27]). It is worth noting, that the stabilizing role of the atmospheres and the oceans were also examined earlier in these systems: in the presence of a dense CO<sub>2</sub> atmosphere and a global ocean, temperature differences can be distributed on the surface [28]. In any case, low-mass stars (where tidal locking occurs frequently) are more prone to violent stellar outbursts in relatively short timescales, therefore disturbing the planet's atmosphere and surface ocean dynamics [29]. For example, this can be the case in the TRAPPIST-1 system, which was originally a promising place to find habitable planets, with liquid water oceans [30].

The strongest correlation on the matrices can be found between the stellar mass—planetary semi-major axis pair ( $r = 0.84$ ). This is an expected correlation originating from the definition of the habitable zone: since main-sequence stars with greater mass have a much larger luminosity ( $L \propto M^3$ ), therefore the zone where a planet can orbit without being too hot, extends further away from the star, with a greater semi-major axis and vice versa.

### 3.2.3. Number of Planets in the System

The inverse correlation between the stellar mass and the number of planets in the star system ( $r = -0.31$ ) seems to support earlier studies [31]. Firstly, the more massive O, B, and A-type stars have short lifetimes (a few million years to a few hundred million years), which are shorter timespans than the evolution of the biosphere on Earth. Additionally, their HZ's edges are advancing outwards much more quickly than the HZ of the lower-main sequence stars, therefore it is hard to determine a stable environment around them. Also, their extreme solar wind is thought to be counter-effective for planet formation [32], since their protoplanetary disc evaporates more quickly.

All in all, to explore the influence of additional planets in a star system on ocean formation, these systems should be examined on a one-by-one basis in further studies.

#### 4. Conclusions

In this study, we mainly focused on the accessible statistical data of the currently confirmed exoplanets and their parent systems, and we created two heatmaps to visualize the connection between exoplanet properties in general, and inside the calculated habitable zones. It can be seen, that the habitable zone definition strengthens the association between the different planetary parameters, and provides information about the connecting features of exoplanetary systems. Also, there are possible associations between the planetary radius/mass and stellar metallicity and multiple characteristics. The such broad association suggests that the mentioned parameters can be possibly used as a proxy, to fine-tune the detection methods for star systems that are more likely to host terrestrial planets hopefully with a global ocean.

#### Author Contributions:

**Funding:** This research received no external funding.

#### Institutional Review Board Statement:

**Informed Consent Statement:** Not applicable.

**Data Availability Statement:** This research has made use of the NASA Exoplanet Archive, which is operated by the California Institute of Technology, under contract with the National Aeronautics and Space Administration under the Exoplanet Exploration Program.

**Conflicts of Interest:** The authors declare no conflict of interest.

#### References

1. Borucki, W.J.; Koch, D.; Basri, G.; Batalha, N.; Brown, T.; Caldwell, D.; Caldwell, J.; Christensen-Dalsgaard, J.; Cochran, W.D.; DeVore, E.; et al. Kepler Planet-Detection Mission: Introduction and First Results. *Science* **2010**, *327*, 977. <https://doi.org/10.1126/science.1185402>.
2. Rauer, H.; Catala, C.; Aerts, C.; Appourchaux, T.; Benz, W.; Brandeker, A.; Christensen-Dalsgaard, J.; Deleuil, M.; Gizon, L.; Goupil, M.-J.; et al. The PLATO 2.0 mission. *Exp. Astron.* **2014**, *38*, 249–330. <https://doi.org/10.1007/s10686-014-9383-4>.
3. Sullivan, P.W.; Winn, J.N.; Berta-Thompson, Z.; Charbonneau, D.; Deming, D.; Dressing, C.D.; Latham, D.W.; Levine, A.M.; McCullough, P.R.; Morton, T.D.; et al. The Transiting Exoplanet Survey Satellite: Simulations of Planet Detections and Astrophysical False Positives. *Astrophys. J.* **2015**, *809*, 77. <https://doi.org/10.1088/0004-637X/809/1/77>.
4. NASA Exoplanet Science Institute. Planetary systems composite table. IPAC: <https://doi.org/10.26133/NEA13>.
5. Piaulet, C.; Benneke, B.; and Almenara, J. Evidence for the volatile-rich composition of a 1.5-earth-radius planet. *Nat. Astron.* **2022**, *1–17*. <https://doi.org/10.1038/s41550-022-01835-4>.
6. Léger, F. Selsis, C. Sotin; et al. A new family of planets? "Ocean-Planets". *Icarus* **2004**, *169*, 499–504. <https://doi.org/10.1016/j.icarus.2004.01.001>.
7. Elkins-Tanton, L.T. Formation of early water oceans on rocky planets. *Astrophys. Space Sci.* **2011**, *332*, 359–364. <https://doi.org/10.1007/s10509-010-0535-3>.
8. Kimura, T.; and Ikoma, M. Predicted diversity in water content of terrestrial exoplanets orbiting M dwarfs. *Nat. Astron.* **2022**, *6*, 1296–1307. <https://doi.org/10.1038/s41550-022-01781-1>.
9. Olson, S.L.; Jansen, M.; Abbot, D.S. Oceanographic Considerations for Exoplanet Life Detection. *Astrophys. J.* **2020**, *895*, 19. <https://doi.org/10.3847/1538-4357/ab88c9>.

10. Schulze-Makuch, D.; Méndez, A.; Fairén, A.G.; Von Paris, P.; Turse, C.; Boyer, G.; Davila, A.F.; Walther-Antonio, M.; Catling, D.; Irwin, L.N. A Two-Tiered Approach to Assessing the Habitability of Exoplanets. *Astrobiology* **2011**, *11*, 1041–1052. <https://doi.org/10.1089/ast.2010.0592>.
11. Dole, S.H. Habitable planets for man. **1970**. <https://doi.org/10.7249/CB179-1>.
12. Kopparapu, R.K.; Ramirez, R.; Kasting, J.F.; Eymet, V.; Robinson, T.D.; Mahadevan, S.; Terrien, R.C.; Domagal-Goldman, S.; Meadows, V.S.; Deshpande, R. Habitable Zones around Main-sequence Stars: New Estimates. *ApJ* **2013**, *765*, 131. <https://doi.org/10.1088/0004-637X/765/2/131>.
13. Kasting, J.F. Runaway and moist greenhouse atmospheres and the evolution of Earth and Venus. *Icarus* **1988**, *74*, 472–494. [https://doi.org/10.1016/0019-1035\(88\)90116-9](https://doi.org/10.1016/0019-1035(88)90116-9).
14. Kasting, J.F. CO<sub>2</sub> condensation and the climate of early Mars. *Icarus* **1991**, *94*, 1–13. [https://doi.org/10.1016/0019-1035\(91\)90137-1](https://doi.org/10.1016/0019-1035(91)90137-1).
15. Gaudi, B.S.; Stassun, K.G.; Collins, K.A.; Beatty, T.G.; Zhou, G.; Latham, D.W.; Bieryla, A.; Eastman, J.D.; Siverd, R.J.; Crepp, J.R.; et al. A giant planet undergoing extreme-ultraviolet irradiation by its hot massive-star host. *Nat* **2017**, *546*, 514–518. <https://doi.org/10.1038/nature22392>.
16. Lissauer, J.J. Planet Formation. *Annu. Rev. Astron. Astrophys.* **1993**, *31*, 129–172. <https://doi.org/10.1146/annurev.aa.31.090193.001021>.
17. Fischer, D.A.; and Valenti, J. The Planet-Metallicity Correlation. *Astrophys. J.* **2005**, *622*, 1102–1117. <https://doi.org/10.1086/428383>.
18. Lineweaver, C.H. An Estimate of the Age Distribution of Terrestrial Planets in the Universe: Quantifying Metallicity as a Selection Effect. *Icarus* **2001**, *151*, 307–313. <https://doi.org/10.1006/icar.2001.6607>.
19. Johnson, J.A.; Aller, K.M.; Howard, A.W., and Crepp, J.R. Giant Planet Occurrence in the Stellar Mass-Metallicity Plane. *PASP* **2010**, *122*, 905. <https://doi.org/10.1086/655775>.
20. Santos, N.C.; Israelian, G.; and Mayor, M. Spectroscopic [Fe/H] for 98 extra-solar planet-host stars. Exploring the probability of planet formation. *Astron. Astrophys.* **2004**, *415*, 1153–1166. <https://doi.org/10.1051/0004-6361:20034469>.
21. Kipping, D.M.; and Sandford, E. Observational biases for transiting planets. *MNRAS* **2016**, *463*, 1323–1331. <https://doi.org/10.1093/mnras/stw1926>.
22. Dressing, C.D.; Spiegel, D.S.; Scharf, C.A.; Menou, K. and Raymond, S.N. Habitable Climates: The Influence of Eccentricity. *Astrophys. J.* **2010**, *721*, 1295–1307. <https://doi.org/10.1088/0004-637X/721/2/1295>.
23. Rodriguez, A. and Ferraz-Mello, S. Tidal decay and circularization of the orbits of short-period planets. *EAS Publ. Ser.* **2010**, *42*, 411–418. DOI: 10.1111/j.1365-2966.2011.18861.x.
24. Rodriguez, A.; and Ferraz-Mello, S. Tidal decay and circularization of the orbits of short-period planets. *ÉAS Publ. Ser.* **2010**, *42*, 411–418. <https://doi.org/10.1051/eas/1042044>.
25. Jackson, B.; Greenberg, R. and Barnes, R. Tidal Evolution of Close-in Extrasolar Planets. *Astrophys. J.* **2008**, *678*, 1396–1406. <https://doi.org/10.1086/529187>.
26. Kite, E.S.; Gaidos, E.; and Manga, M. Climate Instability on Tidally Locked Exoplanets. *Astrophys. J.* **2011**, *743*, 41. <https://doi.org/10.1088/0004-637X/743/1/41>.
27. Wordsworth, R. Atmospheric Heat Redistribution and Collapse on Tidally Locked Rocky Planets. *Astrophys. J.* **2015**, *806*, 180. <https://doi.org/10.1088/0004-637X/806/2/180>.
28. Wordsworth, R.D.; Forget, F.; Selsis, F.; Millour, E.; Charnay, B.; Madeleine, J.-B. Gliese 581d is the First Discovered Terrestrial-mass Exoplanet in the Habitable Zone. *Astrophys. J.* **2011**, *733*, L48. <https://doi.org/10.1088/2041-8205/733/2/L48>.
29. Dong, C.; Huang, Z.; Lingam, M.; Tóth, G.; Gombosi, T.; Bhattacharjee, A. The dehydration of water worlds via atmospheric losses. *Astrophys. J.* **2017**, *847*, L4. <https://doi.org/10.3847/2041-8213/aa8a60>.
30. Vida, K.; Kóvári, Z.; Pál, A.; Oláh, K.; Kriskovics, L. Frequent Flaring in the TRAPPIST-1 System Unsuitable for Life?. *Astrophys. J.* **2017**, *841*, 124. <https://doi.org/10.3847/1538-4357/aa6f05>.
31. Kennedy, G.M., and Kenyon, S.J. Planet Formation around Stars of Various Masses: The Snow Line and the Frequency of Giant Planets. *ApJ* **2008**, *673*, 502–512. <https://doi.org/10.1086/524130>.
32. Veras, D.; Tremblay, P.-E.; Hermes, J.J.; McDonald, C.H.; Kennedy, G.M.; Meru, F.; Gänsicke, B.T. Constraining planet formation around 6–8 M stars. *MNRAS* **2020**, *493*, 765–775. <https://doi.org/10.1093/mnras/staa241>.

**Disclaimer/Publisher’s Note:** The statements, opinions and data contained in all publications are solely those of the individual author(s) and contributor(s) and not of MDPI and/or the editor(s). MDPI and/or the editor(s) disclaim responsibility for any injury to people or property resulting from any ideas, methods, instructions or products referred to in the content.